Journal of the European Ceramic Society 19 (1999) 939–944

PII: S0955-2219(98)00349-5
0955-2219/98/$ - see front matter

High Temperature Optical Absorption Spectroscopy at Pure and Y-doped $BaCeO_3$

H. Huck, P. Ehrhart* and W. Schilling

IFF, Forschungszentrum Jülich GmbH, D-52425 Jülich, Germany

Abstract

The defect induced optical absorption has been investigated at different oxygen partial pressures and at temperatures up to 800°C for the high temperature protonic conductor $BaCeO_3$. Thin films of pure and 10 mol% Y-doped $BaCeO_3$ with thickness up to 11μm have been deposited on transparent MgO single crystal substrates by means of RF-magnetron sputtering techniques. After separating the different contributions to the optical absorption we have concentrated on the part of the spectra which is attributed to free small polarons. Under reducing external gas atmospheres these polarons are generated in the film along with oxygen vacancies and contribute to the electronic conductivity by their hopping processes. We report on time resolved measurements of the defect reaction kinetics after a change of the external gas atmosphere and investigate the influence of the doping atoms by comparing $BaCe_{0.9}Y_{0.1}O_{3-\delta}$ and $BaCeO_3$. The observations are discussed in terms of the diffusion behavior of the oxygen vacancies. © *1999 Elsevier Science Limited. All rights reserved*

Keywords: films, spectroscopy, electrical conductivity, perovskites.

1 Introduction

Rare earth doped $BaCeO_3$ has attracted much attention due to its possible applications as a protonic conductor e.g. in fuel cells or gas sensors.[1] $BaCeO_3$ crystallizes in the perovskite structure and can be doped with rare earth ions which substitute mainly Ce^{4+} ions[2] and are electrically compensated by the formation of oxygen vacancies. Therefore the doped material may be dominated by oxygen ionic conduction in dry oxygen atmospheres and change to a protonic conductor in wet atmospheres. In addition to this ionic conductivity an electronic conductivity may arise under reducing gas atmospheres where additional oxygen vacancies are formed which must electrically be compensated by electrons. As the corresponding electronic conductivity may shortcut the ionic conductivity, which is the basic property for the above mentioned applications, the formulation of the relevant defect equilibria must be known in detail. These electronic properties can be investigated by optical spectroscopy in-situ at high temperature and in continuation of previous work[3] we report here first results on the defect kinetics during changes of the atmospheres.

In order to separate the different mechanisms for the generation of oxygen vacancies we compared pure and doped samples. This comparison directly allows for conclusions on the underlying defect equilibria. For the 10% Y doped samples vacancies are introduced according to the charge neutrality requirements

$$Y_2O_3 \leftrightarrow 2Y' + 3O_o^x + V_o^{\cdot\cdot} \qquad (1)$$

Additional vacancies can be created at low oxygen partial pressures by the reduction of the material,

$$O_o^x \leftrightarrow 1/2O_2(g) + V_o^{\cdot\cdot} + 2e' \qquad (2)$$

These electrons seem to be localized at the Ce^{4+} sublattice forming free small polarons, Ce^{3+}, and can be detected by optical absorption spectroscopy.[3,4] As these electrons are directly related to the additional vacancies [eqn (2)], the formation of these vacancies can be detected by optical absorption. A possible additional introduction of electrons along with the incorporation of hydrogen: $H_2(g) + 2O_o{}^x \leftrightarrow 2OH_o^{\cdot} + 2e'$, seems unlikely for the present conditions[5] and is neglected in the following discussion. As the vacancies can similarly be

*To whom corresponence should be addressed. Fax.: +49-2461-61-2550; e-mail: p.ehrhart@kz-juelich.de

formed in the pure $BaCeO_3$ we can follow the formation and diffusion of vacancies by changing the oxygen partial pressure at high temperatures for both materials. Hence, the comparison of the differently doped samples may yield some information on the basic questions of possible influence of defect complex formation at high concentrations of vacancies and/or doping atoms. This complex formation may influence the defect equilibria as well as the diffusion behavior.

2 Experimental Methods

Pure $BaCeO_3$ as well as 10 mol% Y-doped $BaCeO_3$ films with thickness between 10 and 11 μm were deposited by RF-magnetron sputtering on MgO (100) substrates. The sputtering gas was a mixture of Ar and 10% of oxygen and the substrate temperature was 550°C. The films were characterized by transmission electron microscopy (TEM),[6] surface profiling, Rutherford backscattering spectroscopy (RBS), and X-ray diffraction (XRD). These films grow initially with a high (001)-texture but with increasing thickness above 1 μm the preferred orientation turns slowly to (110). The chemical composition is close to the target composition and there were no indications of foreign phases from the XRD data, however, Raman spectra show some indication for the presence of small amounts of CeO_2.

The optical absorption spectra were measured in the wave length region between 200 and 1000 nm with the sample in a special furnace described elsewhere.[7] Well defined oxygen partial pressures $p(O_2)$ were established by flowing water vapor saturated H_2/N_2 mixtures at a total pressure of 1 atmosphere. The water vapor partial pressure was controlled by the temperature of the water bubbler.

The quantity determined from the experiment is the absorption coefficient, α, which is defined as $\alpha = \ln(I_0/I)/d$ where I_0 is the intensity of the incoming light, I that of the transmitted light and d is the sample thickness. Spectra were measured at temperatures between 600 and 800°C and Fig. 1 shows typical examples. The spectra can be separated into three contributions: first an absorption background which corresponds to the perfect, defect free crystal and includes reflection losses at the surface, secondly the strong increase of the absorption close to the band-gap energy which can be described by a disorder induced Urbach tail[7] and thirdly a broad maximum which can be attributed to electrons in the form of small polarons. This latter contribution is a measure of the electron concentration and will be investigated in the following. In order to observe changes within the time scale of seconds this part of the spectrum was measured simultaneously by using an imaging spectrograph and a linear array of Si diodes.

The polaron absorption can be quantitatively described (for details see [4]):

$$\alpha_{\mathrm{FSP}} = \alpha^0[(1-\exp(-E/kT))/(E/k\mathrm{T})]X \exp - \{(E-4E_h)^2/(16E_hkT+\Gamma^2)\} \quad (3)$$

E = photon energy, k = Boltzmann factor, T = Temperature, $E_h = E_a - \Gamma^2/24\,kt$; E_a is the activation energy for small polaron hopping and Γ considers an additional broadening due to the distribution of localized energy levels of the polarons. From a fit of the observed line position and shape of the FSP band the thermal activation energy for the polaron hopping (and the additional parameter Γ) can be deduced.[3]

Assuming a Gaussian line profile which is a reasonable approximation here[4] we can approximate the FSP absorption by a Smakula type formula: by considering the absorption in the maximum, α^*_{FSP}, the width of the band, ΔE_{FSP}, and the oscillator strength, f, of the transition the electron concentration is determined:

$$[e'] = 9 \times 10^{16}(n/(n^2+2)^2)(1/f)\alpha^*_{\mathrm{FSP}}\Delta E_{\mathrm{FSP}} \quad (4)$$

n denotes the refractive index. Unfortunately the oscillator strength is not known for the FSP transition in $BaCeO_3$, therefore we will consider here only relative changes of the electron concentration.

3 Experimental Results

Figure 2 shows examples of the built up and the decay of the FSP absorption upon a change of the ambient oxygen partial pressure. After switching from a nitrogen atmosphere to a hydrogen atmosphere we observe a fast increase and—within the experimental uncertainties—the approximation at a saturation value of the absorption. After reversing to nitrogen a corresponding decrease is observed and these changes are completely reversible and can be cycled for many times. The amount of the change depends on the temperature. The similar behavior of the pure and the yttrium doped samples show directly that the stoichiometric vacancies are not involved in the process and that the processes are essentially dominated by the equilibrium indicated in eqn (2).

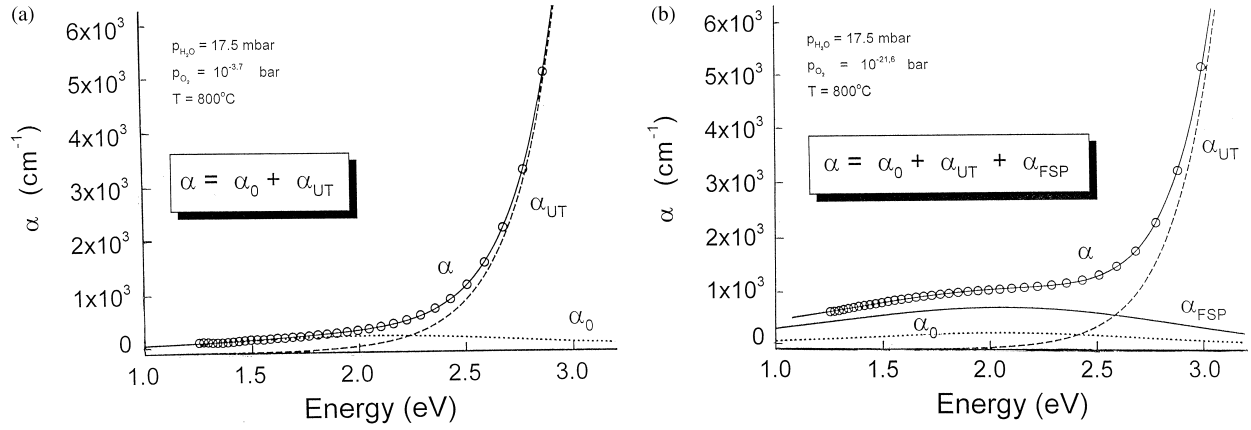

Fig. 1. Absorption spectra of $BaCe_{0.9}Y_{0.1}O_{3-\delta}$ at 800°C and for different oxygen partial pressures. The experimental data points are fitted by a model considering the general background, α_0, the Urbach tail, α_{UT}, and the scattering by the free small polarons, α_{FSP}. (a) $p(O_2) = 10^{-3.7}$ bar, $p(H_2O) = 17{\cdot}5$ mbar and (b) $p(O_2) = 10^{-21.6}$ bar, $p(H_2O) = 17{\cdot}5$ mbar; the essential change is the appearance of the broad FSP absorption band.

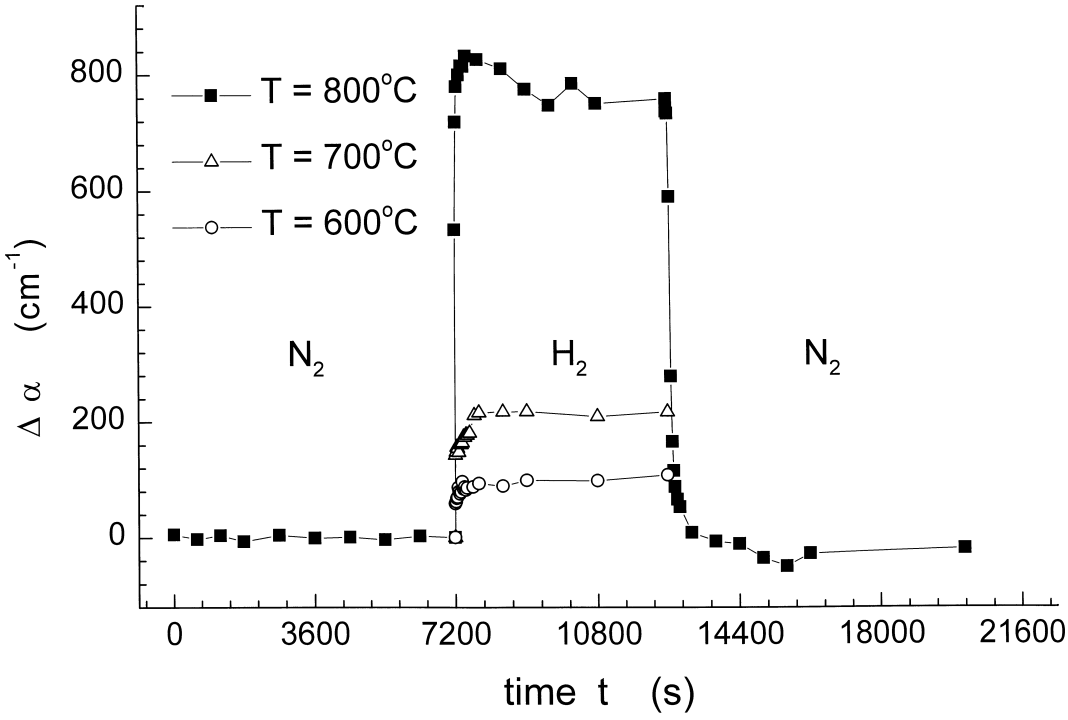

Fig. 2. Change of the absorption coefficient due to the FSP as a consequence of the change of the atmosphere nitrogen–hydrogen–nitrogen. Data points are taken at the maximum of the FSP absorption at 2.1 eV and are shown for pure $BaCeO_3$ at temperatures of 600, 700 and 800°C.

Figure 3 shows the details of kinetics of the built up and decay of the FSP absorption on a shorter time scale. All examples refer to a measuring temperature of 700°C. In addition to the experimental points different model calculations for the diffusion limited charging and decharging reactions are plotted for comparison. These calculations are performed for the model of a thin platelet which is open from one side only[8] as the MgO substrate is assumed to be completely unaffected at the given temperatures. For the given boundary conditions we can express the time dependent average concentration $< c(t) >$ within the platelet in the form of a series expansion:

$$\frac{< c(t) > - c(0)}{c(\infty) - c(0)} = 1 - \frac{8}{\Pi^2} \sum_{n=0}^{\infty} \frac{1}{(2n+1)^2} \exp\left[-(2n+1)^2 \frac{t}{\tau}\right] \tag{5}$$

$c(0)$ and $c(\infty)$ are the initial defect concentration and the saturation value respectively. τ is the relaxation time and is related to the diffusion coefficient, $D : \tau = 4d^2/(\pi^2 D)$. As the average concentration is directly proportional to the measured average absorption coefficient, α, the relaxation time, τ, can be determined from a fit of eqn (5) to

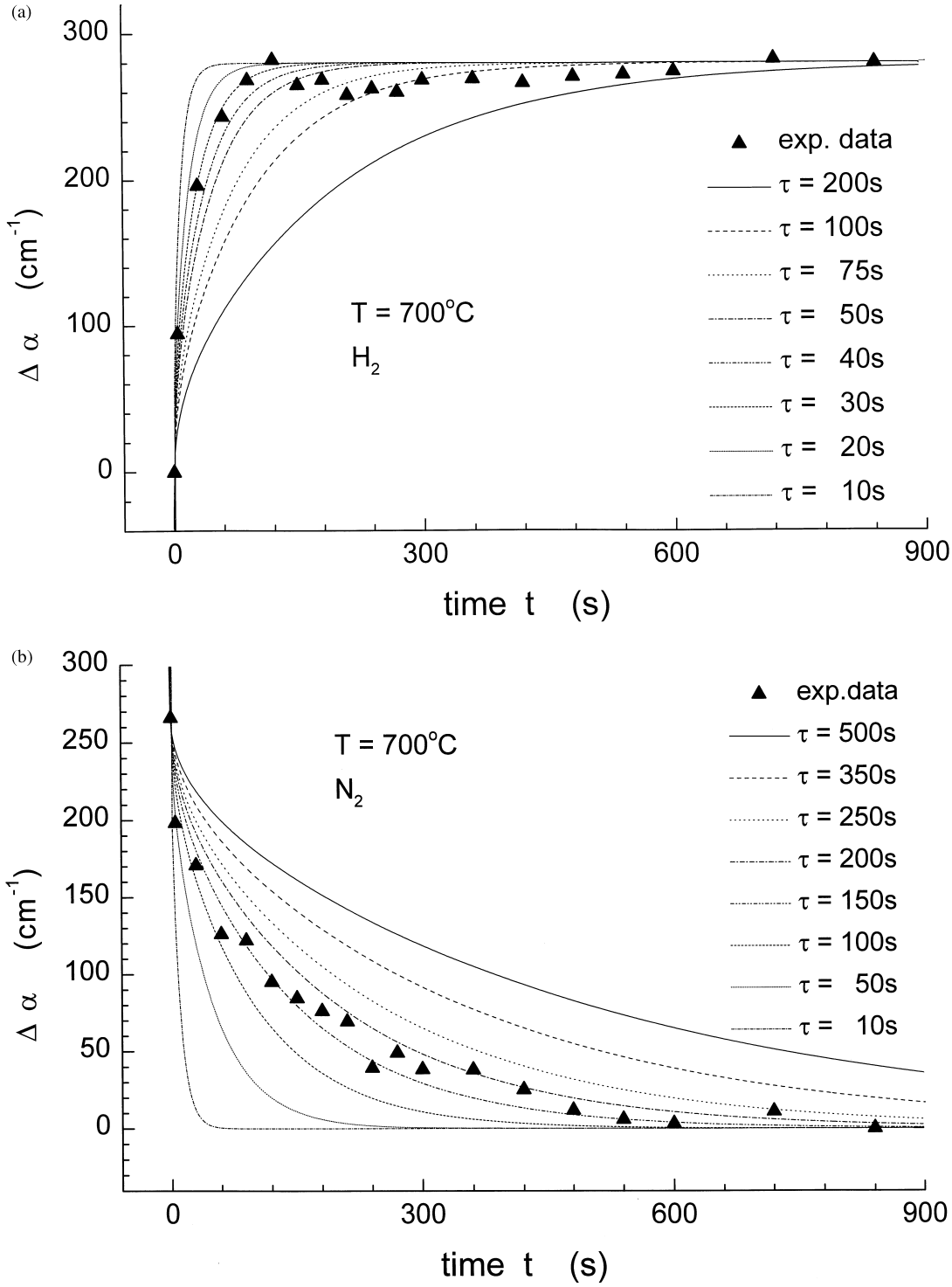

Fig. 3. Kinetics of the (a) growth and (b) decay of the FSP band for $BaCe_{0.9}Y_{0.1}O_{3-\delta}$ at a measurement temperature of 700°C. The different lines correspond to the diffusion limited charging and de-charging reaction for a thin platelet (11 μm) from one side. The parameter τ is the relaxation time.

the experimental data. After long times the first few terms in eqn (5) yield a sufficiently good approximation, but in order to obtain a good approximation also for short times we included the first 16 terms into the calculations shown in Fig. 3.

The good qualitative description of the time dependence of the charging reaction, (H_2), indicates a diffusion limited reaction and the best fit of the parameter, τ, yields finally the diffusion constant, D. We observed a similar behavior for both types of samples, however, the decharging reaction (N_2) indicates a slower reaction and a lower quality fit. This behavior might be attributed to the slower removal of the hydrogen from the sample atmosphere and similar observations have been reported[9] for $SrCeO_3$. Therefore we consider in the following only the charging reaction.

The observed effective diffusion constants are summarized in an Arrhenius diagram in Fig. 4. The values for D are in reasonable agreement with the

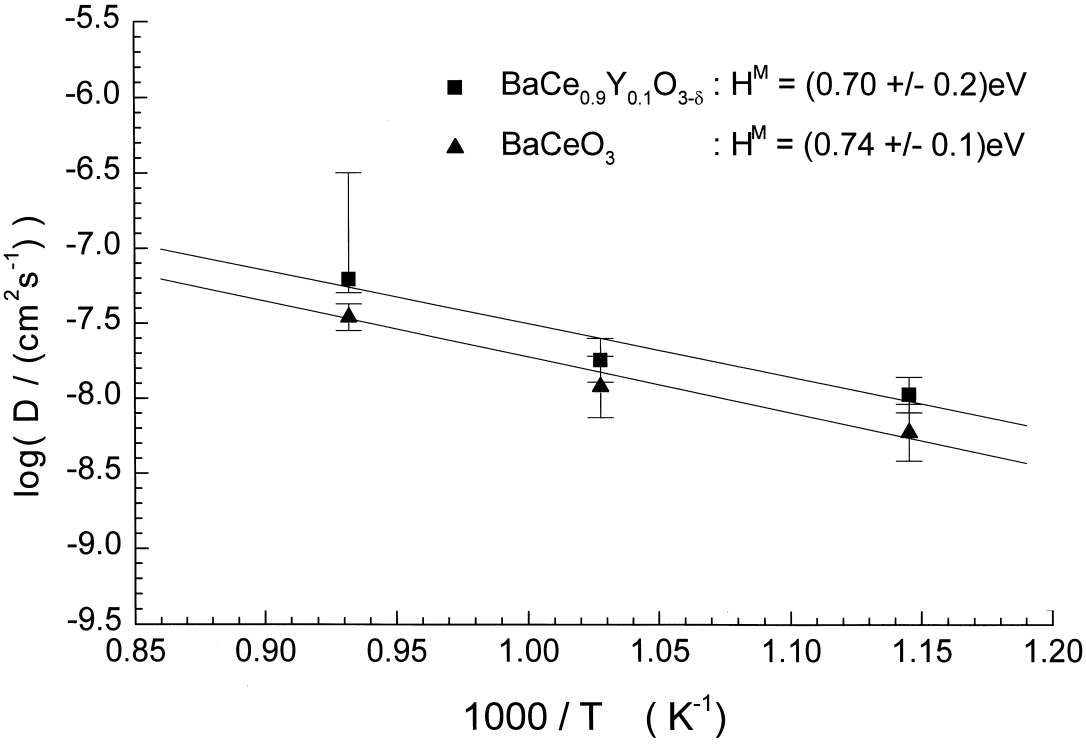

Fig. 4. Arrhenius plots of the diffusion coefficients in pure and 10% Y-doped $BaCeO_3$.

values of the oxygen diffusion[10] in Gd–doped $BaCeO_3$, however, they must be considered as chemical diffusion coefficients. We will discuss here only the activation energies which represent the activation energy for vacancy migration, H^M, as the oxygen diffusion is attributed to vacancies on the oxygen sublattice. Although the diffusion coefficient for the doped sample seems to be systematically somewhat higher than that of the undoped sample there is no relevant difference for the activation energy within the given error bars.

4 Conclusion

We have demonstrated that the optical absorption due to small polarons in $BaCeO_3$ can be used for time resolved measurements of the defect reaction kinetics after a change of the external gas atmosphere. As the change of the polaron concentration can be assumed to be directly related to the concentration of oxygen vacancies the diffusion behavior of the oxygen vacancies could be investigated.

The activation energy for the diffusion of oxygen vacancies is determined to $H^M = 0{\cdot}72 \pm 0{\cdot}2$ eV. This value is in reasonable agreement with conclusions from measurements of the electrical conductivity for 19% Y doped single crystals[11] which yielded a value of 0·71 eV. Similar values are also observed for different doping atoms in $BaCeO_3$ (for Gd doped samples values between 0·69 eV [12] and 0·79 eV [10,12] have been reported), as well as for yttrium doped CeO_2($H^M = 0{\cdot}67$ eV[13]).

The influence of the doping atoms has been investigated by comparing $BaCe_{0.9}Y_{0.1}O_{3-\delta}$ and pure $BaCeO_3$. Remarkably the observed activation energy for vacancy migration is not affected by the presence of the doping atoms and the large amount of compensating vacancies (5%). This observation means that there is no indication of defect interactions. Hence, these results give no support to the assumption of a decrease of the activation energy with decreasing vacancy concentration.[12]

Acknowledgements

The authors thank H.-J. Bierfeld and Dr P. Meuffels for their valuable support in the sputter deposition of the perovskite films.

References

1. Iwahara, H., Esaka, T., Uchida, H. and Maeda, H., Proton conduction in sintered oxides and ist application to steam electrolysis for hydrogen production. *Solid State Ionics*, 1981, **3/4**, 359–363.
2. Nowick, A. S. and Du, Y., High-temperature protonic conductors with perovskite-related structures. *Solid State Ionics*, 1995, **77**, 137–146.
3. He, T. and Ehrhart, P., An optical in-situ study of $BaCeO_3$ at high temperatures. *Solid State Ionics*, 1996, **86–88**, 633–638.

4. He, T., Optical absorption of free small polarons at high temperatures. *Phys. Rev.*, 1995, **B51**, 16689–16694.
5. Bonanos, N., Transport properties and conduction mechanism in high-temperature protonic conductors. *Solid State Ionics*, 1992, **53/56**, 967.
6. He, T., Jia, C. L., Ehrhart, P. and Meuffels, P., On the preparation and microstructure of Y-doped $BaCeO_3$ perovskite thin films. *Solid State Ionics*, 1996, **89**, 9–12.
7. He, T., Ehrhart, P. and Meuffels, P., Optical band gap and Urbach tail in Y-doped $BaCeO_3$. *J. Appl. Phys.*, 1996, **79**, 3219–3223.
8. Fromm, E. and Gebhardt, E., *Gase und Kohlenstoff in Metallen*. Springer, Berlin–Heidelberg–New York, 1976.
9. Kosacki, I. and Anderson, H. U., The structure and electrical properties of $SrCe_{0.95}Yb_{0.05}O_3$ thin film protonic conductors. *Solid State Ionics*, 1997, **97**, 429–436.
10. Kreuer, K. D., Schönherr, E. and Maier, J., Proton and oxygen diffusion in $BeCeO_3$ based compounds: A combined thermal gravimetric analysis and conductivity study. *Solid State Ionics*, 1994, **70/71**, 278–284.
11. Kreuer, K. D., Dippel, Th., Baikov, Yu. M. and Maier, J. Water solubility, proton and oxygen diffusion in acceptor doped $BaCeO_3$: A single crystal analysis. *Solid State Ionics*, 1996, **86/88**, 613–620.
12. He, T., Kreuer, K. D. and Maier, J., Impedance spectroscopic study of thermodynamics and kinetics of a Gd-doped $BaCeO_3$ single crystal. *Solid State Ionics*, 1997, **95**, 301–308.
13. Nowick, A. S., Atom transport in oxides of the fluor8ite structure. In *Diffusion in Crystalline Solids*, ed. G. E. Murch and A. S. Nowick. Academic Press, New York, 1984 1993, p. 143–188.